ELSEVIER

Thermochimica Acta 392–393 (2002) 195–207

thermochimica acta

www.elsevier.com/locate/tca

Multi-frequency heat capacity measured with different types of TMDSC

P. Kamasa[a,c], M. Merzlyakov[b], M. Pyda[a,c], J. Pak[a,c], C. Schick[b], B. Wunderlich[a,c,*]

[a]*Department of Chemistry, The University of Tennessee, Knoxville, TN 37996-1600, USA*
[b]*Department of Physics, University of Rostock, Universitätsplatz 3, D-18051 Rostock, Germany*
[c]*Oak Ridge National Laboratory, Chemical and Analytical Sciences Division, Oak Ridge, TN 37831-6197, USA*

Received 11 December 2000; accepted 17 April 2001

Abstract

The heat capacities of sapphire (Al_2O_3) and sodium chloride (NaCl), have been measured to establish the accuracy and precision of two different temperature-modulated differential scanning calorimeters operated in diverse multi-frequency modes. The calorimeters have then been applied to find the apparent, reversing heat capacity of polystyrene as a function of frequency in the glass transition region. The first modulation mode consisted of a series of linear heating and cooling segments and produced four harmonics with practically equal temperature amplitudes (1st, 3rd, 5th, and 7th), one of lower amplitude (9th), and almost negligible higher harmonics. The second modulation mode is a rather sharp step ending in an isotherm or slow temperature-decrease and leads to a controlled spike in the heat-flow rate response which produces Fourier components of similar amplitudes for all harmonics of the rates of changes of temperature. The apparent, reversing heat capacity is evaluated from the amplitudes of the heat-flow rates and the corresponding sample temperatures or heating-rates. A time-constant or calibration constant which accounts for thermal conductivities and resistances within the calorimeters can be evaluated from the different harmonics of each run. Measurements in the glass transition region have a slow response of the sample. They are evaluated by separating the sample effect from the calorimeter response which can be extrapolated from data gained outside the transition. One measurement is thus sufficient for the evaluation of the frequency dependence of the heat capacity in the glass transition region.

Keywords: Heat capacity; Glass transition; Temperature-modulated differential scanning calorimetry; TMDSC; Fourier transformation; Higher harmonics; Multi-frequency modulation

1. Introduction

The invention [1] of temperature-modulated differential scanning calorimetry (TMDSC) had a profound impact on the measurement of time-dependent thermal properties. Among many other applications, this method enables to provide data on the frequency-dependence of heat capacity, as it is observed in the glass-transition region [2]. These experiments to evaluate the frequency-dependence, however, require multiple runs through the temperature region of interest. The multiple-frequency measurements proposed in the present research allow to use one experiment for the evaluation of the effect of several frequencies.

* Corresponding author. Tel.: +1-865-675-4532; fax: +1-865-675-4532.
E-mail address: wunderlich@chartertn.net (B. Wunderlich).

0040-6031/02/$ – see front matter
PII: S0040-6031(02)00102-8

This permits an exact correspondence of the sample history for all frequencies, a condition which cannot be guarantied in separate experiments.

Measurements with different modulation frequencies were proposed earlier [1], but first applied extensively to the calibration of TMDSC for high precision heat capacities. In the case steady state is not reached during a calorimetric experiment, one must consider that significant temperature gradients exist within sample and reference calorimeters, and the individual thermal resistances and thermal conductivities of sample, reference and calibration runs must be assessed [3]. The multi-frequency modulation was in this first discussion accomplished with a four-frequency sawtooth of 14 segments. Heat capacities of a precision approaching 0.1% could be demonstrated for all three common commercial scanning calorimeters (T.A. Instruments [4], Mettler-Toledo [5], and Perkin-Elmer [6]). A different modulation program, which also leads to multi-frequency data, is the step-isotherm modulation. In its simplest form it consists of a series of isotherms, interrupted by a periodic, step-wise increase or decrease of the temperature [7]. In this paper, both methods are tested with measurements of the heat capacities of Al_2O_3, and NaCl and applied to the evaluation of the frequency dependence of the reversing heat capacity in the glass transition range of polystyrene. The four-frequency sawtooth method is used with a TA Instruments MDSC™ 2920, the step-isotherm is carried out with a Perkin-Elmer Pyris-1™. The results of the similarities and differences in modulations and calorimeters are discussed with the goal to optimize future TMDSC.

2. Experimental detail

2.1. Four-frequency sawtooth measurements

In standard differential scanning calorimetry (DSC) quantitative experiments are usually carried out after steady state has been reached, i.e. all points in the twin calorimeters are expected to change their temperature with the same rate $q = \mathrm{d}T/\mathrm{d}t$. The programmed temperature is usually a linear ramp over a rather large temperature interval (typically 2–200 K) with heating rates of 5–40 K min^{-1}, and measurements can be made from temperatures between 100 and 1000 K [8]. The difference in temperatures between reference and sample ($T_\mathrm{r} - T_\mathrm{s} = \Delta T$) is directly proportional to the heat-flow rate Φ, so that

$$C_p = \frac{\Phi}{q} K, \tag{1}$$

where K is obtained by calibration with a calorimetric standard, such as sapphire (Al_2O_3). A typical precision of up to 3% is possible [8].

In TMDSC, the programmed temperature is produced by superposition of a constant heating rate and a temperature-modulation [9,10]. The constant, underlying heating-rate corresponds to the sliding average over ±1/2 modulation period and is written as $\langle q \rangle$. The initial modulations applied to TMDSC were sinusoidal and measurements were carried out under conditions which remained close to steady state, even during the modulation. Many measurements were made in the quasi-isothermal mode, i.e. without an underlying heating rate $\langle q \rangle = 0$ [11,12].

In the quasi-isothermal method of TMDSC, a reversing heat capacity can be evaluated from the amplitudes of the heat-flow rate A_Φ and the corresponding sample temperature, $A_{T\mathrm{s}}$ [12]:

$$C_p = \frac{A_\Phi}{A_{T_\mathrm{s}}\omega} K(\omega), \tag{2}$$

where ω is the frequency in rad s^{-1} ($2\pi/t_\mathrm{p}$, with t_p representing the modulation period in s) and $K(\omega)$ corrects for the different modulation in the reference calorimeter ($K(\omega) = [1 + (C_\mathrm{r}\,\omega/K)^2]^{0.5}$, with C_r representing the heat capacity of the reference calorimeter and K, the Newton's law constant). Note that $A_{T\mathrm{s}}\,\omega$ is the amplitude of the heating rate, A_q. The amplitudes are extracted from the raw data, gathered as a function of time, by finding the first harmonic of the Fourier-transform into the frequency-domain. All extraneous heat losses which are different in frequency from ω are thus eliminated, improving the quality of the measurement. It was also shown that for TMDSC with an underlying heating rate $\langle q \rangle$, Eq. (2) could also be used in a pseudo-isothermal analysis by subtracting the total or underlying effects, as for example for heat-flow rate by forming at any time t difference $\Phi(t)_\mathrm{reversing} = \Phi(t) - \langle \Phi(t) \rangle$. This method is feasible as long as the calorimeter remains in steady state and $\langle \Phi(t) \rangle$ is constant or changes linearly [12].

Many applications of the TMDSC method need to provide data on the frequency-dependence of heat capacity, as it is observed in the glass-transition region [2,13]. These experiments require multiple runs through the temperature region of interest. The multiple-frequency measurements proposed for the present research allow to use *one* experiment for the evaluation of the effect of several frequencies. This permits an exact correspondence of the sample history for all frequencies, a condition which cannot be guarantied in separate experiments. Measurements of heat capacities with different modulation frequencies were proposed earlier [1], but first applied extensively to a detailed calibration of TMDSC as mentioned in Section 1 [3]. A sawtooth modulation was created and data of the first harmonic ($v = 1$), as well as for higher harmonics of the sawtooth were used for the analysis ($v = 3, 5, 7, \ldots$). By adjusting Eq. (2) for different frequencies, one obtains [14]:

$$C_p = \frac{A_\phi(v)}{A_{T_S}(v)v\omega} K(v\omega). \tag{3}$$

In analogy to Eq. (2), the dimension-less correction function $K(v\omega)$ in Eq. (3) can be written as

$$K(v\omega) = \sqrt{1 + \tau^2(v\omega)^2}, \tag{4}$$

where τ is an empirical constant. A sawtooth modulation introduces abrupt changes in temperature and can thus never keep the calorimeter in steady state, so that τ must correct for effects of instrument design, sample and reference properties such as thermal conductivity, mass, and contact resistances. At higher frequencies τ may even lose its constancy with ω.

A centrosymmetric, quasi-isothermal sawtooth about T_0, i.e. a modulation without an underlying heating rate, $\langle q \rangle = 0$, can be described by the Fourier series

$$T(t) - T_o = \frac{8A}{\pi^2}\left(\sin\omega t - \frac{1}{9}\sin 3\omega t + \frac{1}{25}\sin 5\omega t - \frac{1}{49}\sin 7\omega t + \frac{1}{81}\sin 9\omega t - \cdots\right), \tag{5}$$

where A is the sawtooth amplitude. Only the first harmonic in Eq. (5) has a big amplitude ($0.81A$), the other amplitudes decrease quickly with frequency, so that the ninth harmonic has an amplitude of only $0.01A$. Calculations of the heat capacities from the higher harmonics should have less precision, surprisingly they were shown to be usable for heat capacity evaluation [15].

In order to improve the evaluation of heat capacity from these higher harmonics, we generated a four-frequency sawtooth with close identical harmonics for $v = 1$, 3, 5, and 7 with a Fourier series which is given by [8]:

$$T_x(t) - T_o = A\big(0.38\sin\omega t + 0.25\sin 3\omega t + 0.22\sin 5\omega t + 0.35\sin 7\omega t - 0.04\sin 9\omega t + 0.01\sin 11\omega t\big) \tag{6}$$

The programming steps of such a sawtooth are presented in Table 1 for an overall period of 420 s (30 s per sub-segment). This simplified four-frequency sawtooth will be applied in this research and analyzed using Eqs. (3) and (4) as discussed earlier [3]. The fifth term of the series is distinctly smaller, but can still be used for the analysis. The sixth and higher terms have only a negligible contribution. The four-frequency modulation for the heat-flux DSC used in this research is obtained from the set of linear heating and cooling segments as displayed in Fig. 1a. Despite the lag of the sample temperature, the resulting rounded sawtooth is described by an equation similar to Eq. (6).

Table 1
Four-frequency sawtooth program for $t_p = 420$ s

Segment no.[a]	Time (s)	Amplitude (K)	Heating rate (K min^{-1})
1	0–15	0.0–1.0	+4
2	15–45	1.0–0.0	−2
3	45–75	0.0–0.5	+1
4	75–105	0.5–0.0	−1
5	105–135	0.0–0.5	+1
6	135–165	0.5–0.0	−1
7	165–195	0.0–1.0	+2
8	195–225	1.0 to −1.0	−4
9	225–255	−1.0–0.0	+2
10	255–285	0.0 to −0.5	−1
11	285–315	−0.5 to −0.0	+1
12	315–345	0.0 to −0.5	−1
13	345–375	−0.5 to −0.0	+1
14	375–405	0.0 to −1.0	−2
15	405–420.0	−1.0–0.0	+4

[a] Note that in order to keep a centrosymmetric sawtooth, segments 1 and 15 are half segments.

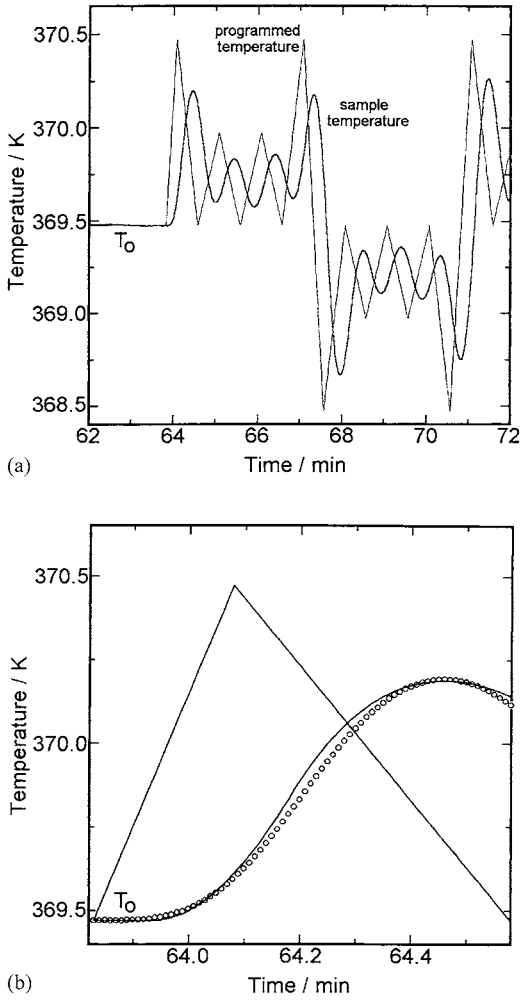

Fig. 1. (a) Temperature program of a single cycle of the four-frequency sawtooth and the actually achieved sample temperature for a 23.623 mg NaCl sample (overall amplitude 1.0 K, period of one cycle 420 s, each segment lasts 30 s); (b) enlargement of the first part of the modulation (⋀) and the calorimeter response (◯) of (a), compared with the response of an equivalent RC electrical circuit (solid curve).

The calorimeter used for the present measurement was a TA Instuments MDSC™ 2920, run in the standard DSC mode, i.e. without making use of the sinusoidal modulation software and corresponding evaluation provided by the manufacturer. The details of the calorimeter are given in the literature [8]. Quasi-isothermal experiments were performed at the base temperatures, T_0. The analysis of the experimental data, consisting of the deconvolution of the various harmonics of the sample temperature and heat-flow rate, as well as the calculation of the heat capacities, C_p, was processed with our own software, programmed in Mathematica 3.0 [4]. The temperature calibration was set with the melting temperatures of indium and water at a heating rate of 10 K min^{-1}. The heat-flow rate was initially set by the heat of fusion of indium and is then corrected with a calibration run with Al_2O_3 (sapphire). Dry nitrogen gas with a flow rate of 20 ml min^{-1} was purged through the DSC cell. The time constant which governs the lag of the sample temperature relative to the program temperature shown in Fig. 1a depends on the heat capacity of the calorimeter and all involved thermal resistances, as well as the thermal conductivity of the sample. In Fig. 1b the sample-temperature response (◯) is given in an enlarged plot for the first heating–cooling segment. The solid curve is obtained from a simple equivalent RC electric circuit from which the time constant can be estimated to be about 15 s. For a more precise match of the temperature function, time delays introduced by the controller and due to the diffusion of the heat from the heater to the sample must be taken into account. Although the reference temperature is not directly available, the construction of the twin calorimeter ensures a similar characteristic of the reference calorimeter. Repeatability of the temperature within the oscillations is reached after one segment of the basic modulation. The faster response of calorimeters with temperature control closer to the heater has been illustrated also, and leads to a more precise match with the programmed sawtooth, as expected [5,6].

2.2. Step-isotherm measurements

Considerably simpler is the programming of the step-isotherm modulation. The temperature and heating-rate profile are schematically drawn in Fig. 2. The reversing heat-flow rate can be seen from Eq. (2) to be proportional to the amplitude of the rate of temperature change ($A_{T_s}\omega = A_q$), and this signal can be derived from a delta function which contains a series of higher harmonics, all of identical amplitudes. One delta-function at (t–t_i) per period, as shown in Fig. 2, can thus be used for the generation of the heat capacity spectrum. The corresponding temperature profile has the indicated step-wise increase in temperature. A slow, underlying heating- or cooling-rate can be

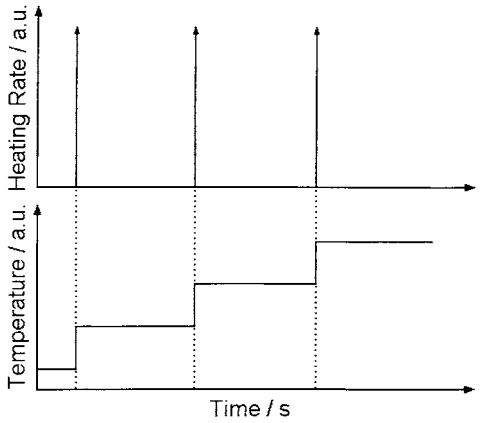

Fig. 2. Upper curve: heating-rate profile consisting of one delta function per period; lower curve: the corresponding temperature–time program to the upper curve.

added between the steps in the temperature–time-program. When necessary the temperature steps can also be negative [7].

The multi-frequency experiment with a step-isotherm temperature profile was carried out with a Perkin-Elmer Pyris 1^{TM} power-compensated DSC. The details of the calorimeter are given in the literature [8]. The example illustrated in Fig. 3 shows the temperature–time profile that was programmed by repetition of two segments, an isotherm of 20 min followed by a heating step of 2.0 K, programmed with a heating rate of 150 K min^{-1} which

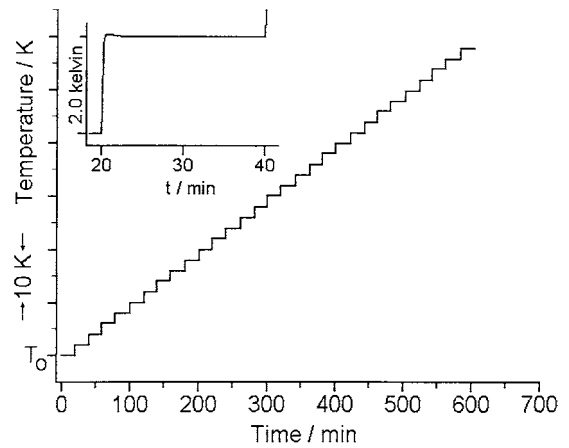

Fig. 3. The temperature–time profile of a complete analysis, consisting of repetition of isothermal heating segments of 2.0 K steps, Perkin-Elmer Pyris 1^{TM} DSC, the inset shows an enlargement of the sample temperature during one step.

leads to heating segments of 0.8 s. The inset shows an enlargement of the sample temperature for one period. One can see that even in the enlarged inset the actually measured temperature follows the programmed temperature closely.

The data treatment was carried out as follows: assuming that k points are obtained per period for the $\Phi(t)$ and $q(t)$ signals, one calculates the apparent heat capacity for the frequency ω as

$$m_s c_p^{\#}(\omega) = \frac{\sum_{i=1}^{k} \Phi_i \cos(\omega t_i) - i\sum_{i=1}^{k} \Phi_i \sin(\omega t_i)}{\sum_{i=1}^{k} q_i \cos(\omega t_i) - i\sum_{i=1}^{k} q_i \sin(\omega t_i)} \quad (7)$$

where m_s is the sample mass and $\omega = 2\pi/t_p$, with t_p representing the period of heating rate or temperature oscillation. The points Φ_i and q_i must be taken with the same sampling rate (number of points per unit time) and be equidistant. The measured heat-flow rate was corrected by subtraction of the baseline for the heat-flow rate. Further, we presented the data of the modulus and argument of $C_p^{\#}(\omega)$, calculated by Eq. (7). For calculations of the apparent heat capacity of the vth harmonic we only substitute ω by $v\omega$ in Eq. (7).

2.3. Samples

The polystyrene used in this research was purchased from Aldrich. Its glass transition temperature is at about 373 K, and the mass-average molar mass is equal to 280,000 Da, measured by size-exclusion chromatography and supplied by the supplier. The Al_2O_3 used for calibration is a standard single crystal of sapphire, traceable to a standard sample of the NBS, dated March 1949 (now National Institute of Standards and Technology (NIST)) with extensive information on its heat capacity [16]. The NaCl was a 99.999% pure single-crystalline granulate (based on metal content), purchased from Puratronic, Inc. (lot no. 22080). Its heat capacity can be found in the literature [17].

3. Results and discussion

3.1. Example data for the four-frequency sawtooth modulation and results on NaCl

Fig. 4 illustrates an example of the measurement and evaluation of the apparent, reversing heat capacity

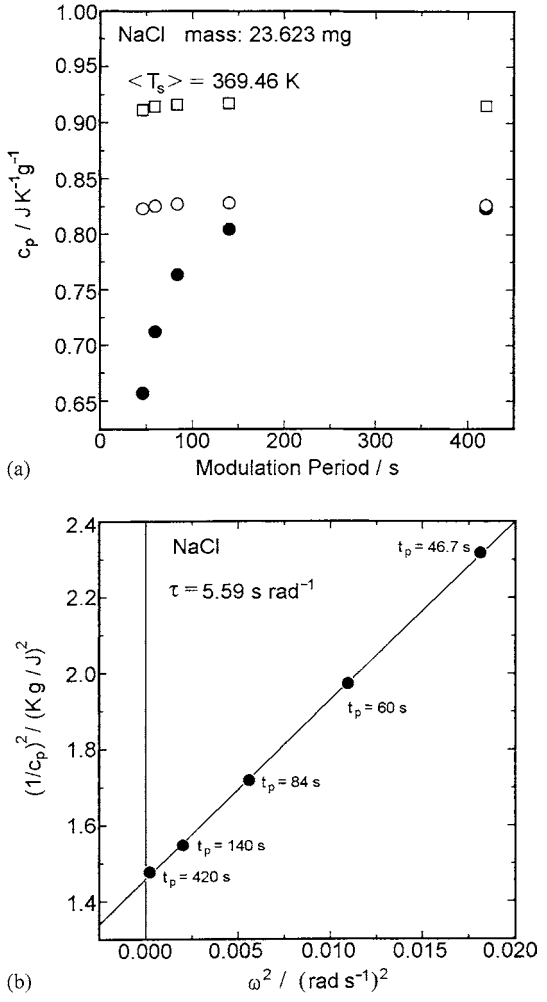

Fig. 4. (a) Heat capacity data for NaCl. Filled circles, uncorrected specific heat capacities calculated with Eq. (3) using $K(v\omega) = 1$. Open circles after correction with Eq. (4). Open squares, the same data as for the open circles, but after correction with the heat capacity of Al_2O_3 (22.762 mg measured under the same conditions as the NaCl); (b) correction-plot for the heat capacities of Fig. 4a. The uncorrected specific heat capacities are plotted as indicated to evaluate τ according to Eq. (4).

of NaCl with the four-frequency sawtooth method ($m_s = 23.623$ mg). The reversing heat capacity represents the absolute value of the reversing heat capacity (also called its modulus), evaluated from Eqs. (3) and (4) for the four main harmonics of the sawtooth of Fig. 1a ($v = 1$, 3, 5, and 7). The 9th harmonic is also included in the evaluation (see Eq. (6)). The uncorrected data gained from Eq. (3) are represented in Fig. 4a by the filled circles. The correction procedure involves the evaluation of τ, as shown in Fig. 4b. The intercept of the plot at $\omega^2 = 0$ is the inverse of the squared heat capacity, corrected for the change with frequency. The calibration of the heat-flow rate with sapphire involved a similar measurement and correction at the same temperature (22.762 mg of Al_2O_3), followed by a parallel shift of the frequency-corrected data to the level given by (□). Typically the four-frequency sawtooth of Table 1 and Fig. 1a was repeated 10 times and checked for repeatability by comparison of their Lissajous figures. Usually only the first cycle showed deviations for the first segment. The data of the 9th cycle were then analyzed.

Fig. 5 shows the results of the measurement of the heat capacity of NaCl using the modulation with a four-frequency sawtooth, as illustrated for one base temperature, T_0, in Fig. 4. Also plotted in the figure are data on NaCl measured with the step-isotherm method of Fig. 3. Three samples, each, of Al_2O_3 ($m_s = 71$ mg) for calibration, and of NaCl ($m_s = 30.7$ mg), were measured in standard aluminum pans of about 25 mg. Both sets of data were compared with data obtained by adiabatic calorimetry [17]. The overall standard deviation of the two DSC sets from the literature is 0.7%, with a clear systematic deviation to lower heat capacities, to be addressed with higher-precision measurements in Section 3.3.

3.2. Example of the step-isotherm modulation and results on $C_p^{\#}$ at the glass transition of PS

Next, a detailed description is given of the evaluation of the apparent heat capacity of polystyrene, as measured with the step-isotherm method, followed by a comparison with similar data from the four-frequency sawtooth measurement. Fig. 6 shows the measured heat-flow rate of a sample-run after subtraction of the baseline heat-flow rate. One can see sharp peaks, which correspond to the very short heating segments with the high heating rate (see Fig. 2). The inset is an enlarged view in the time scale of two neighboring heat-flow-rate peaks. Note that time-axis has a break and the deviation from the baseline is completed in about 30 s.

The calorimeter cannot fully realize the steep heating-rate increase required by the modulation shown in Fig. 2. As a result, the heating-rate amplitudes of the

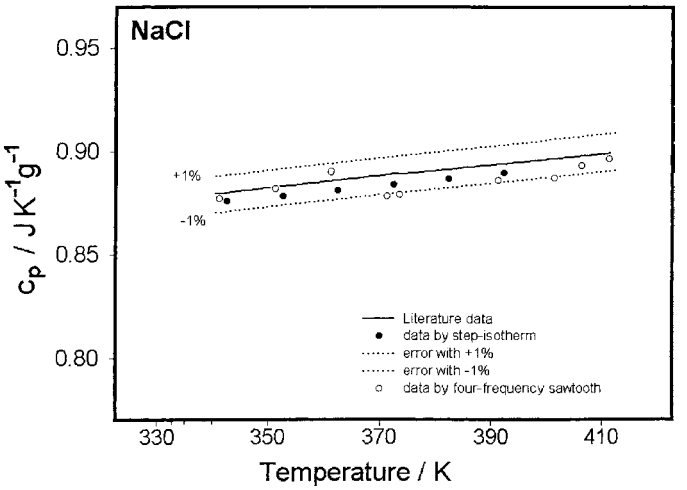

Fig. 5. Heat Capacity of NaCl. Comparison of literature data (—) [17] with the step-isotherm (●) and four-frequency sawtooth (○) data measured with temperature profiles as shown in Figs. 1a and 3 (see also Fig. 6).

Fourier series decrease towards higher frequencies, as is shown in Fig. 7. The figure reveals that the heating-rate amplitude stays practically constant for about one decade of frequency, as expected for a delta function given in Fig. 2.

For the data analysis, first the apparent heat capacity was calculated using Eq. (7). From a single step in the temperature, we calculated the uncorrected, apparent reversing heat capacity $C_p^{\#}(\omega)$ up to the 100th harmonic of the modulation (frequency = 0.083 Hz, modulation period $t_p = 12$ s). Then we applied calibration factor $B_2(\omega)$ [18] to get corrected apparent reversing heat capacity ($C_{p,\text{corrected}}(\omega) = C_{P,\text{measured}}(\omega) \times B_2(\omega)$).

In case one does not expect a frequency dependence of the heat capacity of the sample, one can try to describe frequency dependence of the measured

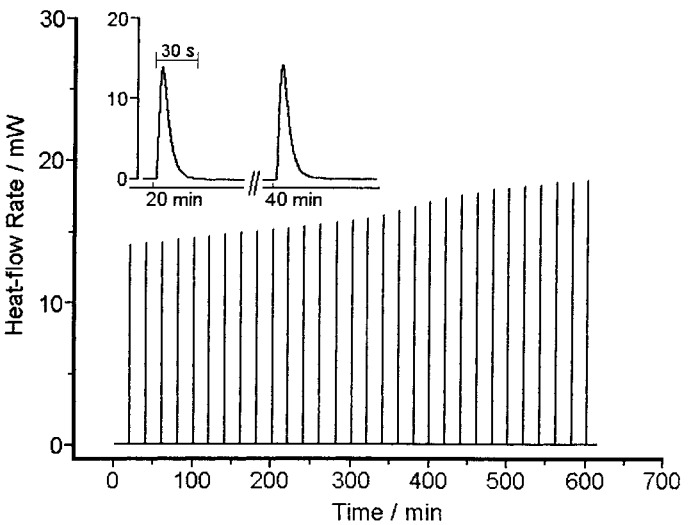

Fig. 6. Heat-flow rate, plotted vs. time of the temperature–time program shown in Fig. 3. Perkin-Elmer Pyris 1^{TM} DSC, polystyrene, sample mass, $m_s = 25$ mg with a standard aluminum pan of about 25 mg.

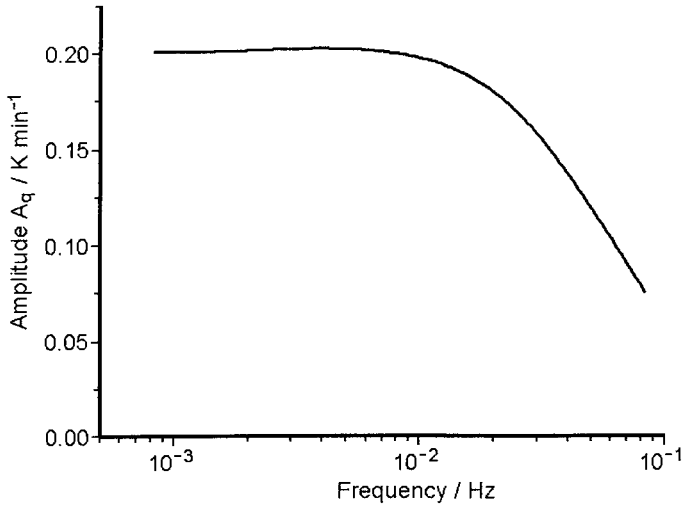

Fig. 7. Change of the heating-rate amplitude as a function of frequency for the temperature–time program, shown in Fig. 3. The heating rate was calculated as the derivative of the sample temperature with time, not of the program temperature. Perkin-Elmer Pyris 1 DSC^{TM}.

apparent heat capacity as manifestation of the heat transfer. As a first approximation, i.e. if one considers only one effective thermal contact K (effective thermal path), $C_p^{\#}(\omega)$ is given by

$$C_p^{\#}(\omega) = \frac{C_p}{1 - (i\omega/K)C_p} \tag{8}$$

In accord with Eq. (8), Fig. 8 shows a plot of $1/C_p^{\#}(\omega)^2$ versus ω^2. The points of $1/C_p^{\#}(\omega)^2$ for different frequencies should lie on a straight line and the slope of the curve equals $1/K^2$. If one takes values of $C_p^{\#}(\omega) = m_s c_p^{\#}(\omega)$ in mJ K^{-1} and ω in rad s^{-1}, the effective thermal contact K will be in mW K^{-1} (compare with Fig. 4b).

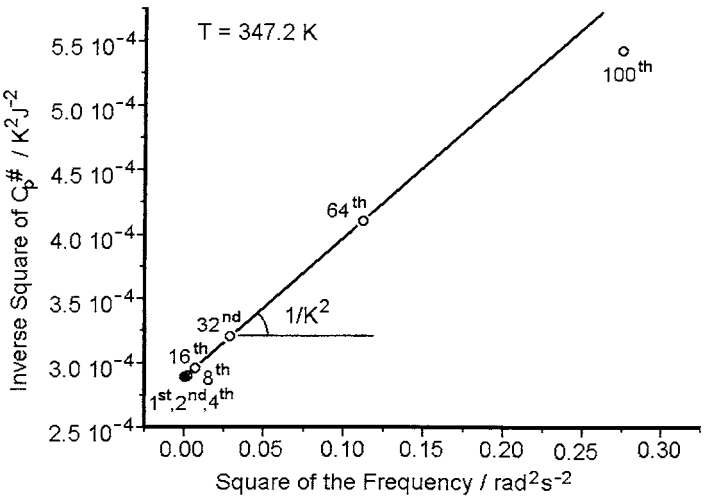

Fig. 8. Plot of $1/C_p^{\#}(\omega)^2$ vs. ω^2. The apparent heat capacity values $C_p^{\#}(\omega)$ were taken after correction by factor $B_2(\omega)$ for the 1st, 2nd, 4th, 8th, 16th, 32nd, 64th, and 100th harmonics. Except the 100th harmonic, the points lie on a straight line. Perkin-Elmer Pyris 1 DSC^{TM}, polystyrene sample, $m_s = 25$ mg with standard aluminum pan of about 25 mg, the mean temperature is 347.2 K (74 °C).

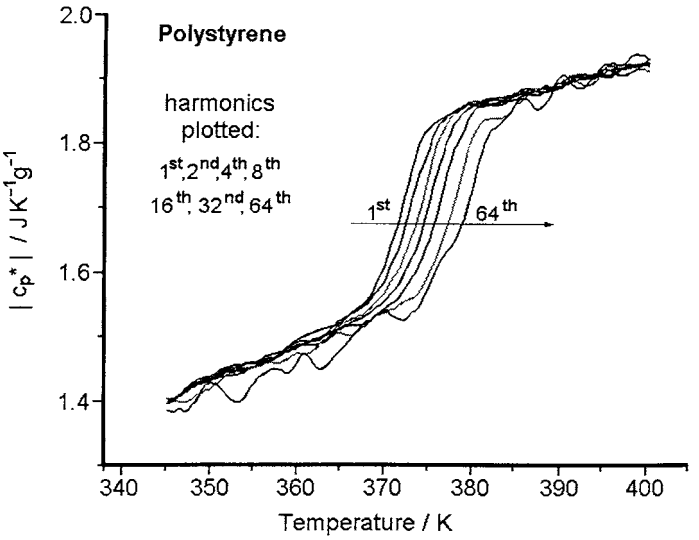

Fig. 9. Modulus of the specific heat capacity of PS vs. temperature in the glass transition region, plotted for different harmonics. The corresponding periods are: 1200.8, 600.4, 300.2, 150.1, 75.0, 37.5, and 18.8 s. Step-isothermal modulation, as shown in Fig. 3. Sample mass $m_s = 25$ mg, modulation period $t_p = 20$ min. Perkin-Elmer Pyris 1 DSC^{TM}.

As seen from Fig. 8, the measured $C_p^{\#}(\omega)$ can be described with one effective thermal contact up to the 64th harmonic. From the slope we determine the effective thermal contact K between the sample and the calorimeter. Outside of the glass transition region, K was about 34 mW K^{-1}. Inside the glass transition the heat capacity of the sample itself depends on frequency and therefore K could not be determined correctly. We assumed in this temperature range the same 34 mW K^{-1} for K.

Eq. (8) is valid for general case when C_p is complex. After determination of K outside the glass transition region, we rewrite Eq. (8) as

$$c(\omega) = \frac{C_p^{\#}(\omega)}{1 + (\mathrm{i}\omega/K)C_p^{\#}(\omega)} \tag{9}$$

and calculated the value of the specific, frequency-dependent heat capacity as $C_p(\omega) = C_p(\omega)/m_s$. The results are shown in Figs. 9 and 10. The 64th harmonic is noisier than lower harmonics because the corresponding heating rate amplitude is smaller, as seen in Fig. 7 (60% of the expected value at low frequency). Outside of the glass-transition region, the heat capacity is real-valued and shows no frequency dependence within experimental uncertainties. Within the glass transition region, the heat capacity is complex and frequency dependent. The curves drawn in Fig. 9 show the typical dynamic glass-transition response of polystyrene. The position of the glass transition is shifted to higher temperature by about 3.5 K on increasing the frequency by one decade, similar to data recorded earlier [19,20].

The analysis by the four-frequency sawtooth modulation in the region of the glass transition of PS is similar to that shown in Fig. 4 for NaCl. Fig. 11 illustrates the values for τ as a function of temperature (see Fig. 4b). Outside the glass transition, τ changes only gradually with temperature. The additional increase is, thus, expected to be due to the slow response of the sample to the change in frequency. The corresponding heat capacities for polystyrene calculated with the τ-values extrapolated through the glass transition region in Fig. 11, and corrected as shown in Fig. 4a, are displayed in Fig. 12. At the point of half increase in the apparent heat capacity, usually taken as the glass transition temperature, T_g, one finds a shift of T_g of about 5 K for an increase in frequency by a factor of 9. This compares to an increase of about 7 K for a change in frequency by a factor of 64 in Fig. 9. Choosing approximately equal changes in t_p for both measurements yields a comparison of 5–4 K, respectively.

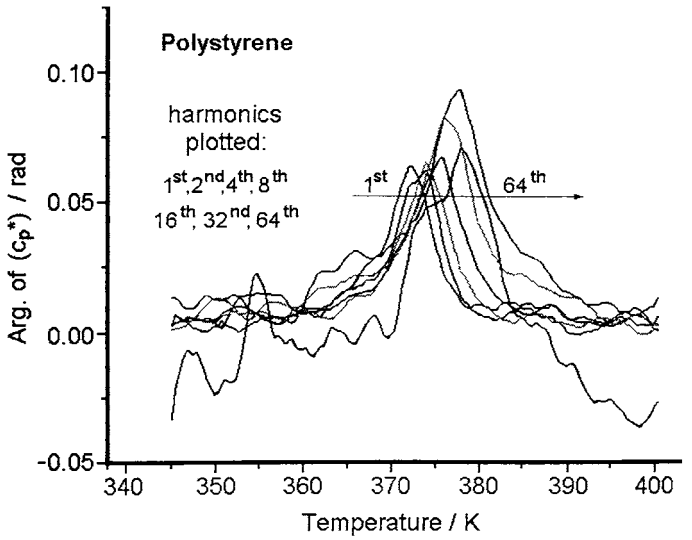

Fig. 10. Argument of the specific heat capacity of PS vs. temperature, plotted for the 1st, 2nd, 4th, 8th, 16th, 32nd, and 64th harmonic. Perkin Elmer Pyris 1 DSC™, Sample mass $m_s = 25$ mg, $t_p = 20$ min.

3.3. Heat capacity measurements with high precision and accuracy

To generate heat capacities of highest precision and accuracy, one can still optimize the conditions of measurement. For example, one can alter the temperature–time profile of Fig. 2 so that (1) the mean temperature does not change, resulting in a quasi-isothermal measurement, (2) the modulation period is reduced, (3) the step is broadened asymmetrically to

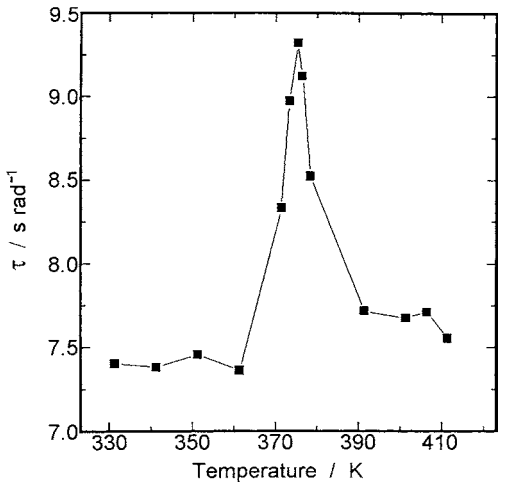

Fig. 11. Change of the value of τ for PS in the glass transition region using the heat-flux MDSC™ 2920 modulated with a four-frequency sawtooth, as shown in Fig. 1. Calculated from the extrapolation using Eq. (4), as illustrated in Fig. 4b. Outside of the glass transition region, the value of τ changes only little, while in the glass transition region the response-time increases as a result of the slow sample response.

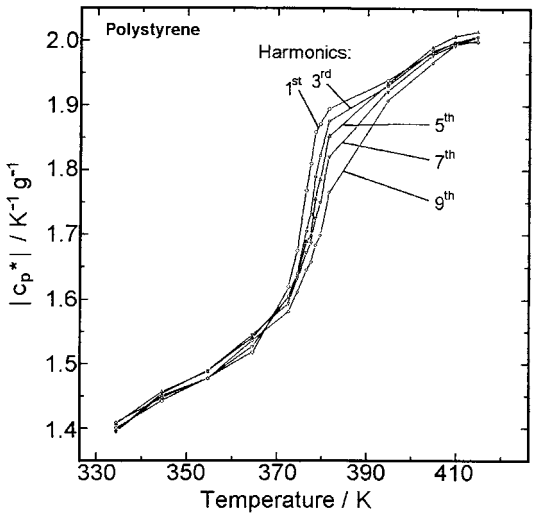

Fig. 12. Modulus of the apparent specific heat capacity of PS vs. temperature in the glass transition region, plotted for different harmonics of the four-frequency sawtooth of Fig. 1. The corresponding periods t_p are: 420, 140, 84, 60, and 46.7 s, TA Instruments MDSC 2920™, mass $m_s = 23.623$ mg, $t_p = 420$ s.

include elements of both a sawtooth and the step-isotherm modulation, (4) the number of repetitive measurements is increased, and (5) larger masses can be used. For each quasi-isothermal measurement, 10 repetitive measurements were made of a heating step of 2 K at a heating rate of 20 K min^{-1}, followed by cooling to the starting temperature to create an asymmetric sawtooth with a modulation period of about 1.0 min. The heating-rate amplitudes of the first few harmonics were about 4 K min^{-1} for this modulation mode. Of these data, we used only the first and second harmonics, to diagram $1/C_p^{\#}(\omega)^2$ versus ω^2 and determine the extrapolated value $1/C_p(0)^2$ (see Fig. 8). With this procedure three samples were analyzed: Al_2O_3 ($m_s = 71$ mg), NaCl ($m_s = 30.7$ mg), and PS ($m_s = 25$ mg), all in standard aluminum pans of about 25 mg. The measured heat capacity of Al_2O_3 was matched to the literature data [16] to derive the calibration factor. The results for the molar heat capacity of NaCl and the specific heat capacity of PS are depicted in Figs. 13 and 14, respectively. The statistical scatter of the measured C_p values for NaCl is about 0.1%, the accuracy is about 0.5%. Most of the deviation from the literature data [17] is clearly a systematical error and needs further investigation. The reproducibility between the two measured sets of data of PS below and above the glass transition gives c_p values which agree to better than 0.2% with the data bank values [21] which are also shown in Fig. 14. The estimated overall accuracy of the data bank was estimated to be only ±3%. The new data suggest that the C_p of PS is considerably more accurate.

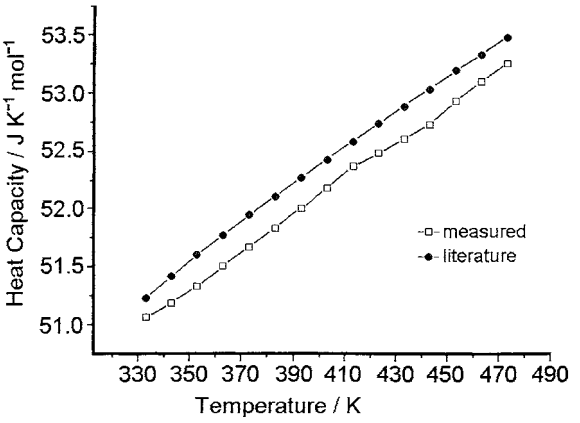

Fig. 13. Molar heat capacity of NaCl vs. temperature. Perkin-Elmer Pyris 1^{TM} DSC, operated with $m_s = 30.7$ mg, $t_p = 1$ min. Literature data from [17].

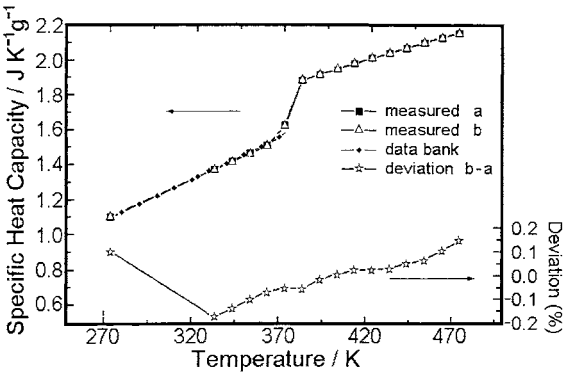

Fig. 14. Specific heat capacity of PS vs. temperature (left ordinate) and the deviations of c_p between two separate measurements (right ordinate). Perkin-Elmer Pyris 1^{TM} DSC, $m_s = 25$ mg, $t_p = 1$ min. Literature data from the ATHAS data Bank [21].

4. Final discussion and conclusions

It is shown that modulation with multiple frequencies is possible in a single experiment. Figs. 4b and 8 prove that the frequency-dependent data can be used to correct for different thermal resistances and conductivities. This correction is essential for experiments which cannot maintain steady state, but can lead to much higher precision by eliminating most heat losses since TMDSC accepts only responses to the fixed modulation frequencies [12]. The need to maintain steady state in TMDSC had limited the precision of heat capacity determinations in the past. The sometimes involved creation of modulation, and always lengthy subsequent data analysis should present no problem, as soon as complete, optimized computer programs become available.

The two modulation methods presented in this paper introduce a series of modifications to multiple frequency operations that can be tailored to the needs for maximum performance of a given DSC. Looking at the modulation in Fig. 3, it is obvious that the sequential step-isotherms could also be looked upon as an asymmetric sawtooth with an underlying heating

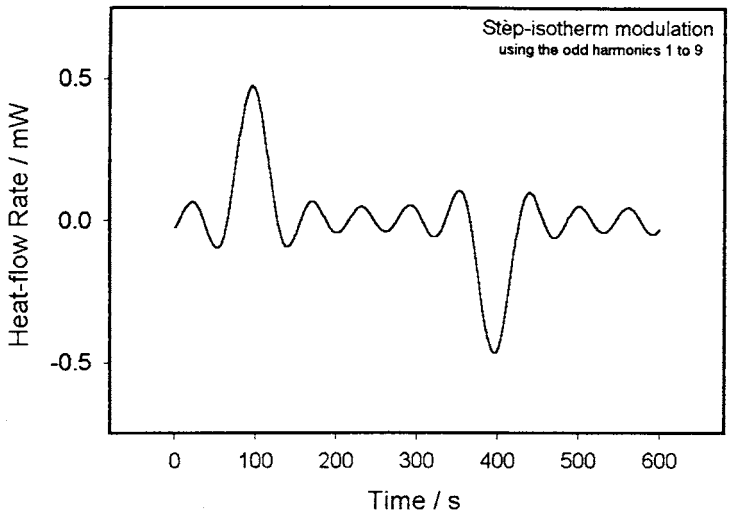

Fig. 15. Heat-flow rate as obtained by adding the 1st, 3rd, 5th, 7th and 9th harmonics of the reversing heat-flow rate for a modulation as in Fig. 3.

rate. Selecting in such an analysis only the experimentally found (pseudo-isothermal) reversing heat-flow rates $\Phi(t)$ of the 1st, 3rd, 5th, 7th, and 9th harmonic and summing them to a five-frequency modulation, one obtains the result shown in Fig. 15. The four-frequency quasi-isothermal modulation of Fig. 1a looks similar in its response, and many further modifications in the designs of step and sawtooth are possible.

In this paper, it could, thus, be shown how the precision and accuracy of heat capacity measurement by DSC can be increased considerably, approaching values usually quoted only for adiabatic calorimetry. This higher precision possibly challenges the literature on thermodynamic data on the well known sample of NaCl with the results in Figs. 5 and 13. It becomes necessary in this case, however, to investigate the reliability of the quoted purity of the sample and its preparation. These are routine requirements for high-precision calorimetry which were in the past of less importance for DSC of limited accuracy.

It is illustrated that relatively simple model calculations, as given in Fig. 1b and by Eq. (8), can be used to describe the correction plots of Figs. 4b and 8. But even if a more complicated functional relationship is needed, as illustrated in the example illustrated in Fig. 16 [5], data of high precision can be obtained. It is obvious that maximum precision has not yet been attained. All run parameters like sample mass, heating rates and their change during modulation, pan weights and thermal contacts to the heater, sample consistency and packing, repetition of measurements, and data analysis could be optimized simultaneously for any given DSC. It is notable, however, that in the present research it was possible to reach comparable data in accuracy and precision with different instruments in different laboratories with different methods.

Figs. 9–12, finally, illustrate that it is also possible with these multi-frequency methods to study the kinetics of transitions. The glass transition was chosen, since in this case it is of importance that the same thermal history exists for the sample while testing with different frequencies. The extraction of the true kinetics of the glass transition, however, still requires considerable work. All presently available theoretical descriptions do not fully describe the data available by TMDSC [22]. Note that differences between Figs. 9 and 12 may also be used to study the interference of the time-scale of an underlying heating rate on the modulation frequencies, as was discovered earlier [23]. Finally, long-term quasi-isothermal TMDSC with multiple frequencies may resolve the change in the kinetics of the glass transition during annealing, and naturally it opens a new avenue for the analysis of the kinetics of the many processes discovered in the melting range of polymers [24].

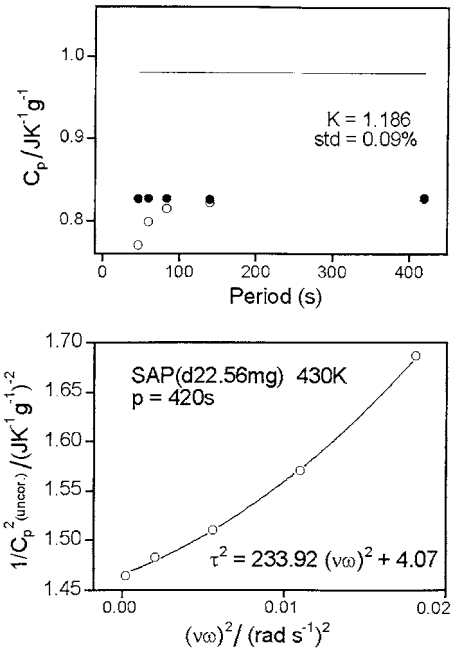

Fig. 16. Heat capacity calibration data with Al_2O_3 (sapphire disc) with the four-frequency sawtooth of Fig. 1. Similar to Fig. 4, but measured with a heat-flux DSC with control close to the heater (Mettler-Toledo DSC 820^{TM}). Open circles, uncorrected specific heat capacities calculated with Eq. (3) using $K(\nu\omega) = 1$. Filled circles, after correction with Eq. (4) as shown in the bottom plot. The correction factor is determined from the distance to the horizontal in the upper plot. Standard deviation 0.09%, $m_s = 22.56$ mg, $t_p =$ 420 s, sample pan 48,551 mg, reference pan 47.426 mg.

Acknowledgements

This work was supported by the Division of Materials Research, National Science Foundation, Polymers Program, Grant No. DMR-9703692 and the Division of Materials Sciences and Engineering, Office of Basic Energy Sciences, US Department of Energy at Oak Ridge National Laboratory, managed and operated by UT-Batelle, LLC, for the US Department of Energy, under contract number DOE-AC05-00OR22725. M. Merzlyakov acknowledges the support from PerkinElmer Instruments USA.

References

[1] M. Reading, B.K. Hahn, B.S. Crowe, Method and Apparatus for Modulated Differential Analysis, US Patent 5 224 775 (1993).
[2] A. Boller, C. Schick, B. Wunderlich, Thermochim. Acta 266 (1995) 97.
[3] B. Wunderlich, R. Androsch, M. Pyda, Y.K. Kwon, Thermochim. Acta 348 (2000) 181.
[4] M. Pyda, Y.K. Kwon, B. Wunderlich, Thermochim. Acta 367/368 (2001) 217, see also Proceedings of the 27th NATAS Conference in Savannah, GA, Vol. 27, 1999, p. 345.
[5] J. Pak, B. Wunderlich, Thermochim. Acta 367/368 (2001) 229, see also Proceedings of the 27th NATAS Conference in Savannah, GA, Vol. 27, 1999, p. 339.
[6] Y.K. Kwon, R. Androsch, M. Pyda, B. Wunderlich, Thermochim. Acta 367/368 (2001) 203.
[7] M. Merzlyakov, C. Schick, Thermochim. Acta 377 (2001) 193.
[8] B. Wunderlich, Thermal Analysis, Academic Press, New York, 1990 (for an update, see the 36 computer-assisted lectures on about 3000 screens, published on the Internet (http://web.utk.edu/~athas/courses/tham99.html), 2000).
[9] P.S. Gill, S.R. Sauerbrunn, M. Reading, J. Therm. Anal. 40 (1993) 931.
[10] M. Reading, A. Luget, R. Wilson, Thermochim. Acta 138 (1994) 295.
[11] A. Boller, Y. Jin, B. Wunderlich, J. Therm. Anal. 42 (1994) 307.
[12] B. Wunderlich, Y. Jin, A. Boller, Thermochim. Acta 238 (1994) 277.
[13] H. Gobrecht, K. Hamann, G. Willers, Journal of Physics E: Scientific Instruments 4 (1971) 21.
[14] R. Androsch, I. Moon, S. Kreitmeier, B. Wunderlich, Thermochim. Acta 357/358 (2000) 267.
[15] R. Androsch, B. Wunderlich, Thermochim. Acta 333 (1999) 27.
[16] D.C. Ginnings, G.T. Furukawa, The heat capacity of synthetic sapphire was measured to high precision by adiabatic calorimetry, J. Am. Chem. Soc. 75 (1953) 522;
D.A. Ditmars, S. Ishihara, S. Chang, G. Bernstein, E.D. Westrum, J. Res., Natl. Bur. Stand. 87 (1982);
D.G. Archer, J. Phys. Chem. Ref. Data 22 (1993) 1441.
[17] M.W. Chase, Jr. NIST-JANAF thermochemical tables, 4th Edition, J. Phys. Chem. Ref. Data, Monograph 9 (1998).
[18] M. Merzlyakov, C. Schick, Thermochim. Acta 330 (1999) 65.
[19] B. Wunderlich, D.M. Bodily, M.H. Kaplan, J. Appl. Phys. 35 (1964) 95.
[20] S. Weyer, A. Hensel, J. Korus, E. Donth, C. Schick, Thermochim. Acta 304/305 (1997) 251.
[21] U. Gaur, B. Wunderlich, J. Phys. Chem., Ref. Data, 11 (1982) 313; see also the ATHAS Data Bank on the Internet (http://web.utk.edu/~athas).
[22] B. Wunderlich, I. Okazaki, Temperature-modulated calorimetry of the frequency dependence of the glass transition of poly(ethylene terephthalate) and polystyrene, in: M.R. Tant, A.J. Hill (Eds.), Structure and Properties of Glassy Polymer, ACS Symposium, American Chemical Society, Washington, DC, Vol. 710, 1998, p. 103.
[23] L.C. Thomas, A. Boller, I. Okazaki, B. Wunderlich, Thermochim. Acta 291 (1997) 85.
[24] B. Wunderlich, A. Boller, I. Okazaki, K. Ishikiriyama, W. Chen, M. Pyda, J. Pak, I. Moon, R. Androsch, Thermochim. Acta 330 (1999) 21.